Structural Analysis of Experimentally Induced Disc Herniation-Like Changes in the Rat

Satoshi Ujigo[1)2)], Daniel Jonsson[1)], Yalda Bogestål[3)], Joakim Håkansson[3)], Jennifer Rosendahl[3)], Lena Brive[3)] and Kjell Olmarker[1)]

1) Musculoskeletal research, Department of Medical Chemistry and Cell Biology, Institute of Biomedicine, Sahlgrenska Academy, University of Gothenburg, Gothenburg, Sweden
2) Department of Orthopaedic Surgery, National Hospital Organization Higashihiroshima Medical Center, Hiroshima, Japan
3) Research Institute of Sweden (RISE), Bioscience and Materials, Borås, Sweden

Abstract:

Introduction: A disc herniation has traditionally been considered as disc tissue that has slipped out from an intervertebral disc. However, it was recently suggested that the disc herniation mass is a product of bioactive substances from the disc and that the disc hernia would more likely be scar tissue than herniated disc material. In this study, we aimed to analyze the structural components of experimentally induced disc herniations and compare with scar tissue and nucleus pulposus, in the rat.

Methods: Twenty-eight rats had their L4-5 discs punctured. After three weeks, the nodule that had been formed over the puncture site, scar tissue from the spine musculature, and normal nucleus pulposus were harvested and processed for further analysis.

Results: Proteomics analysis demonstrated that the formed nodule was more similar to scar tissue than to nucleus pulposus. Gene expression analysis showed that there was no resemblance between any tissues when looking at inflammatory genes but that, there was a clear resemblance between the nodule and scar tissue when analyzing extracellular matrix-related genes. Analysis of the GAG and polysaccharide size distribution revealed that only the nodule and scar tissue contained the shorter versions, potentially short chain hyaluronic acid that is known to induce inflammatory responses. The hematoxylin and eosin stained sections of the nodule, disc tissue, and scar tissue indicated that the morphology of the nodule and scar tissue was very similar.

Conclusions: The nodule formed after experimental disc puncture, and that resembles a disc hernia, has a more structural resemblance to scar tissue than disc tissue. The nodule is, therefore, more likely to be induced by disc-derived bioactive substances than being formed by herniated disc material.

Keywords:

Spine, Intervertebral disc, Disc herniation, Scar tissue, Rat

Spine Surg Relat Res 2020; 4(2): 117-123
dx.doi.org/10.22603/ssrr.2019-0010

Introduction

Disc herniation is a well-known clinical condition ever since 1934 when it was first reported[1)]. At first, it was described as a "slipping" of the disc, but later, it has been referred to as a herniation. The general assumption seems to be that this hard nodule in some way penetrates the annulus fibrosus and then exerts mechanical deformation of an adjacent nerve root. However, it appears unreasonable to think that a hard or semi-hard tissue could penetrate through an annular tear. When performing experimental disc incisions *in vivo,* both in rats and pigs, the gelatinous nucleus pulposus slowly leaks out through the incision[2,3)]. The thought occurred that a disc herniation, as seen at radiologic imaging or by direct inspection in the operating wound, might have another origin than previously described. It was thereby sug-

Corresponding author: Kjell Olmarker, kjell.olmarker@gu.se
Received: February 7, 2019, Accepted: June 17, 2019, Advance Publication: July 10, 2019

gested that the disc herniation mass could be the result of the leakage of disc fluid through the annular tears and by the formation of a hypertrophic scar induced by bioactive substances from the disc tissue. This hypothesis was further corroborated in a study using experimental disc incision in rat[4,5]. Following incision of the annulus fibrosus, the gelatinous nucleus pulposus leaked out into the spinal canal, but within one minute, it was completely liquefied. The epidural space over the incision was thus empty when closing the wound. After 14 weeks, the spinal canal was reopened and a nodule had been formed over the disc incision that resembled a disc herniation. To expand our knowledge of the nature of the formed nodule, we performed an extended assessment of the structural components of the nodule, in order to find out if the nodule was to be considered to be a scar or disc tissue.

Materials and Methods

The animal experiments were performed after prior approval from the local Ethics Committee for Animal Studies at the Administrative Court of Appeals in Gothenburg, Sweden. Female Sprague-Dawley rats (220-230 g, Charles River, Stockholm, Sweden) were used and housed with free access to pellets and water. Room temperature was kept at 21°C with a light schedule of 12 h of daylight starting at 6:00 AM and 12 h of darkness starting at 6:00 PM. Anesthesia was induced and maintained by inhalation of isoflurane (Vetflurane, Virbac, Kolding, Denmark). A single subcutaneous injection of 0.05 mg/kg buprenorphine (Temgesic®, Indivior, Berkshire, UK) was administered preoperatively for additional per- and postoperative analgesia.

A total of 28 rats underwent experimental disc puncture. A midline skin incision over the lumbar spine was made, the thoracolumbar fascia was incised, and the spinal muscles were dissected to expose the left facet joint between the 4th and the 5th lumbar vertebrae. The facet joint was removed to expose the 4th lumbar dorsal root ganglion, the 5th lumbar nerve root, and the intervertebral disc between the 4th and 5th lumbar vertebrae. The L4-5 discs were punctured using a 0.4 mm diameter injection needle. A total of 0.2 ml of air was injected into the disc to facilitate leakage of nucleus pulposus[3,6]. The spinal muscles were sutured, and the skin was closed with metal-clips.

After three weeks, the rats were re-anesthetized and euthanized by cutting the heart, causing the rat to quickly bleed to death while still deeply sedated. The spine was carefully dissected, and tissue samples were collected for the analyses.

From each rat, the following tissue samples were obtained:

- The nodule formed on the surface of the punctured disc (N).
- Scar tissue from the healed incision of the thoracolumbar fascia (S).
- Nucleus pulposus from a non-operated, adjacent disc (D).

1) Proteomics analysis

To obtain sufficient material for analysis, tissue from two rats were pooled and analyzed as one sample. Thus, the following samples were collected for proteomic analysis: Nodule tissue (n = 3), Scar tissue (n = 3), and Nucleus Pulposus (n = 3). The samples were washed in PBS (Phosphate-buffered Saline), snap-frozen in liquid nitrogen, and stored at −80°C. The nodule and nucleus pulposus samples were lysed in 20 µl lysis buffer (2% SDS, 50 mM TEAB) and the scar tissue samples were homogenized and lysed in 300 µl lysis buffer. Protein concentration was determined using Pierce BCA Protein Assay Reagent (Thermo Scientific, Gothenburg, Sweden).

Relative quantitation with isobaric labeling (Tandem Mass Tag, Gothenburg University, Sweden) was used to compare the abundance of peptides and their corresponding proteins. An equal amount of protein from each sample was digested into peptides by mixing it with Trypsin. The peptides were subjected to isobaric-mass-tagging reagents with a unique tag for each sample. The samples were combined, resulting in one or several 10-plexed sets. Relative quantification was performed using Proteome Discoverer (Thermo Scientific, Gothenburg, Sweden). Each tag contained a characteristic reporter ion with a unique structure, which is detectable upon fragmentation. The intensity of these ions was used for quantitation. Only peptides unique for the specific protein were considered.

2) Gene expression analysis

To obtain sufficient material for analysis, tissue from six rats were pooled and analyzed together. The two samples were washed in PBS, snap-frozen in liquid nitrogen, and stored at −80°C. All samples were homogenized using a steal bead and Tissuelyser (Qiagen, Hilden, Germany) at 25 Hz and 5 × 2 min. The supernatant was extracted with the RNeasy Mini Kit (Cat no 74104, Qiagen), including DNase treatment, according to the manufacturer's instructions. The concentration and purity of the extracted RNA samples were analyzed on a spectrophotometer (DropSense96, Trinean, Unchained Labs, Boston, USA). The quality of the RNA was analyzed on gel electrophoresis (Bioanalyzer, Agilent Technologies, Santa Clara, USA).

All samples were reversely transcribed into cDNA using TATAA Grandscript cDNA Synthesis kit #A103 (TATAA Biocenter A, Gothenburg, Sweden). Reverse transcription was performed in 20 µl reaction volumes on T100 (Bio-Rad Laboratories Inc, Berkeley, USA).

All samples were diluted 11 times after reverse transcription. qPCR was performed with TATAA SYBR® GrandMaster Mix #TA01 (TATAA Biocenter AB) and ran in duplicates in 10 µl reactions on CFX384 (Bio-Rad Laboratories Inc) on pre-spotted plates; Acute inflammatory response (R384), extracellular matrix (ECM) and adhesion molecules (SAB Target list) R384 (Bio-Rad Laboratories Inc). The pipetting was performed by a pipetting robot (EpMotion 5070, Eppendorf,

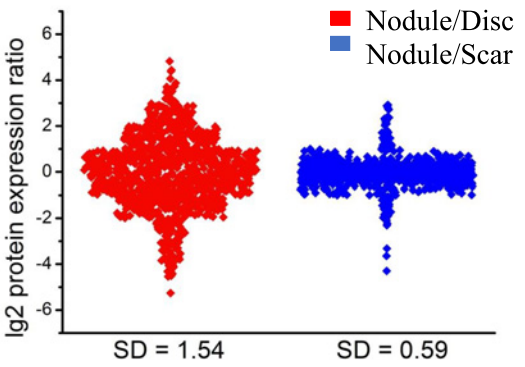

Figure 1. Relative comparison of peptide expression hits identified in proteomics analysis. The expression levels are illustrated as Log2. Equal expression of a peptide in both tissues compared gives the expression ratio 0. Whereas, a higher peptide expression level in the nodule tissue compared with the other tissue results in ratio>0, and a lower peptide expression level in the nodule tissue compared with the other tissue gives ratio<0. There is less difference in relative expression levels between the nodule tissue and disc tissue compared with the difference in relative expression levels between the nodule tissue and scar tissue.

Germany). A two-step temperature program, at default settings from Bio-Rad, was applied and detection was performed in the SYBR channel. Positive control was added to the plates in equal amounts after robot-pipetting.

Data analyses of the two panels were performed separately. For both panels, a reference gene screen was made in order to find the best suitable reference genes. All genes with missing data and Cq values > 34 were removed. In the full data set, genes with more than 50% missing data were removed, and the remaining missing data were replaced with the maximum Cq value plus three cycles for the calculations. The data were normalized against the best suitable reference genes, the lowest expression was set to 1, and the data was then log2.

3) Glycosaminoglycan (GAG) and polysaccharide size distribution

To obtain sufficient material for analysis, tissue from five rats were pooled and analyzed as one sample. Two different experimental series were performed. The first one was designed as a pilot study to illustrate that released polysaccharides were detectable and that the result could be compared between the different samples (nodule, scar, and disc). The second experiment was then performed according to the same protocol to verify the initial observations.

The samples were washed in PBS, snap-frozen in liquid nitrogen, and stored at −80°C. All tissues were rinsed with acetone and lyophilized.

The *O*-linked GAGs were released by beta-elimination under reducing and denaturating conditions. The solubilized materials were then separated by size-exclusion chromatography and detected by UV and refractive index, (SEC/UV/RI). Two sets of experiments were performed at two different time points, using the same protocol. The samples were lyophilized overnight, and the weight was taken before and after lyophilization. The lyophilized tissues were rinsed with 1 ml of ice-cold acetone for 15 min, centrifuged for at 20817 × g for 15 min at 4°C, and the precipitate was dried under vacuum overnight. The samples were extracted with 100 µl (200 µl for scar tissue) of GAG extraction solution (0.5% SDS, 0.1 M NaOH and 0.1% $NaBH_4$) for 16 h at room temperature with constant shaking. The solutions were neutralized by the addition of 20 µl (40 µl for scar tissue) of 1 M potassium acetate and 30 µl (60 µl for scar tissue) of 1 M HCl. Non-solubilized material was removed by centrifugation (15 min, 20817 × g, 4°C). The polysaccharide material was precipitated by the addition of 0.7 ml (1.4 ml for scar tissue) of ethanol (99.8%) saturated with potassium acetate and kept at 4°C for 16 h. The precipitates were recovered after centrifugation (15 min, 20817 × g, 4°C) and repeatedly rinsed with 1 ml ethanol. The final precipitate was lyophilized overnight. Before analysis, the polysaccharides were solubilized in 100 µl (200 µl for scar tissue) 0.1 M phosphate buffer, pH = 7.4. The LC system (Agilent 1220 Infinity) was equipped with a UV- (Agilent 1260 Infinity) and a RI detector (Agilent C1362A). The column used for separation according to size was a PSS Suprema 100 10 µ (8 × 300 mm). The eluent was phosphate buffer pH = 7.4 at a flow rate of 0.5 ml/min.

4) Histology

Disc-, nodule-, and scar tissues were harvested and fixed in 4% paraformaldehyde, washed in PBS, stored in 70% ethanol, and embedded in paraffin. The disc tissue and nodule tissue were decalcified in Ethylenediaminetetraacetic acid. The sections were stained with hematoxylin and eosin.

Results

All rats tolerated the surgical intervention well and gained weight as could be expected.

1) Proteomics analysis

In total, 1080 hits were identified using relative mass spectroscopy. Relative comparison between the three tissue types showed a higher correlation between scar tissue and nodule tissue as compared with disc tissue and nodule tissue displayed as a lower standard deviation in the scar/nodule cluster (Fig. 1).

2) Gene expression analysis

Reference gene analysis was performed using Genorm. The reference genes were selected based on the genes that were most stable in all samples, regardless of the type of tissue. As a result, *Stat3* was selected as a reference gene for the inflammatory gene panel, and *Ctnb1*, *Lamc1,* and *Ecm1*

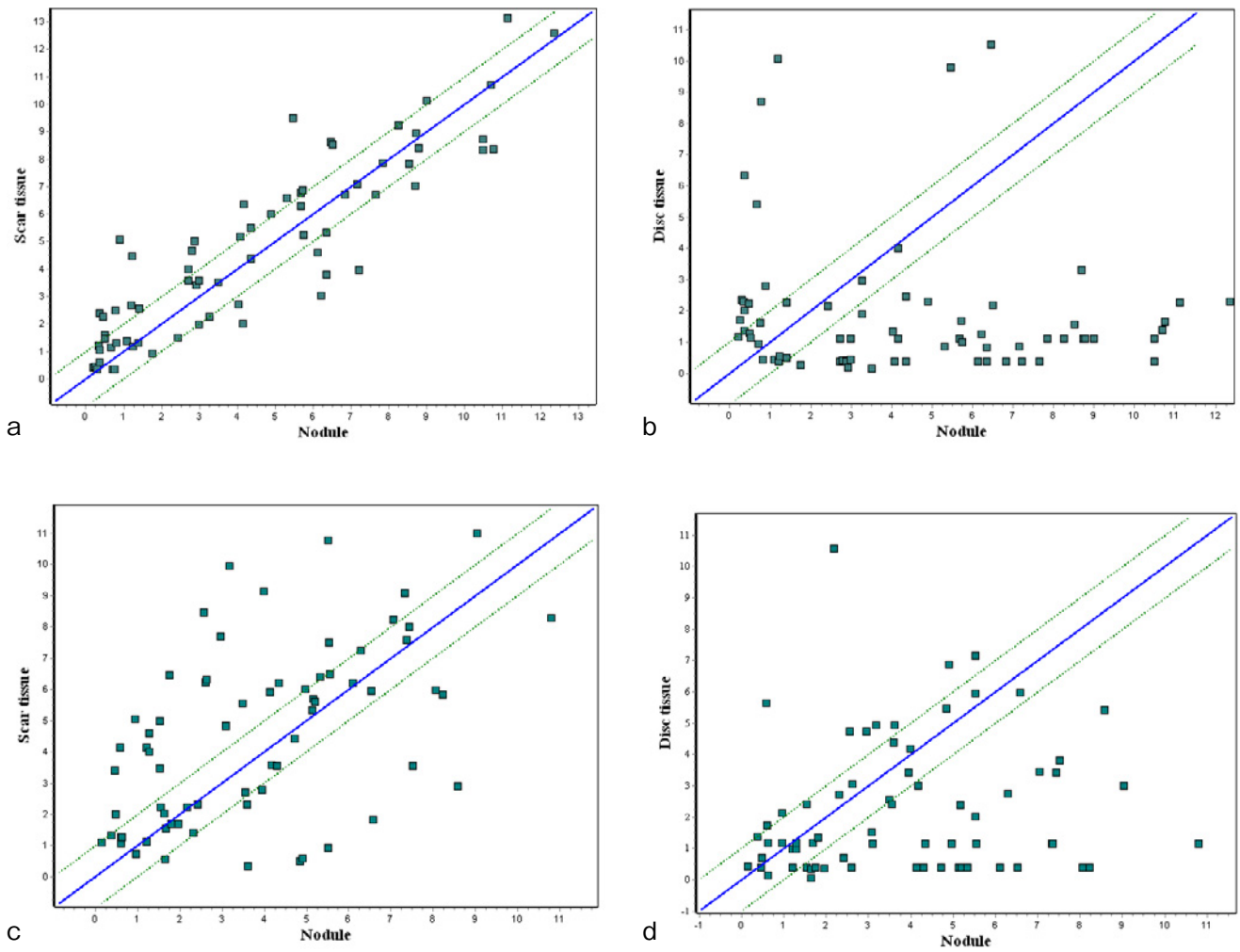

Figure 2. a) Correlation plot of the gene expression levels in the scar tissue samples and the nodule samples showing good correlation (correlation coefficient=0.90) between the ECM and adhesion molecule gene panel and b) from disc tissue samples and the nodule samples showing no correlation (correlation coefficient=−0.11) between the samples. c) Correlation plot of the gene expression levels from the inflammatory gene panel from scar tissue samples and the nodule samples showed no correlation (correlation coefficient=0.53) between the samples d) as well as for the disc tissue samples and the nodule samples (correlation coefficient=0.17). Each dot represents the expression level from one gene. The scales in the x- and y-axis of the graphs indicate gene expression fold change normalized against the reference genes, set as 1.

were selected as reference genes for the ECM and cell adhesion molecule gene panel (data not shown). The gene expression of all other genes was normalized against the expression of the reference genes (set as 1). Correlation plot of the genes expression showed that there was a good correlation (correlation coefficient = 0.9) between the scar tissue samples and the nodule samples on the ECM and adhesion molecule gene panel (Fig. 2a), but no correlation (correlation coefficient = −0.11) between the disc tissue samples and the nodule samples (Fig. 2b). No correlation (correlation coefficients = 0.53 and 0.17, respectively) could be confirmed between any of the tissues for the inflammatory gene panel (Fig. 2c, d).

3) GAG and polysaccharide size distribution

The size distribution of the GAG and polysaccharides from the ECM of two sets of tissues were examined. The amount of each pooled set of tissue is listed in Table 1. The scar tissues were by far the largest pieces, whereas one of the disc tissue samples were below determinable weight, approx. 5 mg, but still visibly present.

Both RI and UV were used as detectors after SEC-separation. The RI is a nonspecific detector and will detect proteins as well as polysaccharides, while the UV detector will not detect polysaccharides but proteins. The RI chromatogram of the two sets of the three different samples, Fig. 3 upper, showed a similarity in profile between the nodule and the disc tissues, whereas the scar tissue in the first experiment showed a different profile. The signals in the chromatograms from both the nodule and the disc tissues were rather weak in intensity as expected when starting with limited amounts. Though the signal present at 12.5 min were present in the chromatograms in both experiments. The scar tissue chromatograms were not as similar between the two

Table 1. Amount of Tissue Used for Size Exclusion Chromatography after Release of *O*-linked Oligosaccharides.

	Experiment 1 mg wet weight	Experiment 2 mg wet weight
Disc tissue	29	not measurable
Scar tissue	156	140
Nodule tissue	18	21

experiments but did include additional signals as compared with the nodule and scar tissues. The similarities between the nodule and the disc tissues were also observable in the UV-chromatograms while the scar tissue again showed a rather different profile (Fig. 3 lower).

The size distributions of polysaccharides were also investigated with the aim of detecting possible shorter chain GAG or polysaccharides potentially involved in the initiation of inflammatory responses to the disc incisions. The scar tissue contained sets of components with molecular weights of 50 kDa or less, observable mainly by RI and less by UV, indicating a polysaccharide-based structure. The disc tissue samples also contain a component observable in the RI-chromatograms in the low molecular weight region with no corresponding signal in the UV-chromatograms. The nodule and scar tissues did not include smaller polysaccharides as compared with the disc tissue, suggesting that no GAG short-chain components were present in unusual excess, potentially causing an inflammatory response.

4) Histology

Analysis of the hematoxylin and eosin stained tissues showed that the nodule tissue was very similar to scar tissue in terms of morphology and cellular structure. Most of the cells in both tissues had fibroblast-like morphology, and both tissues also contain a significant amount of ECM-like structures, Fig. 4.

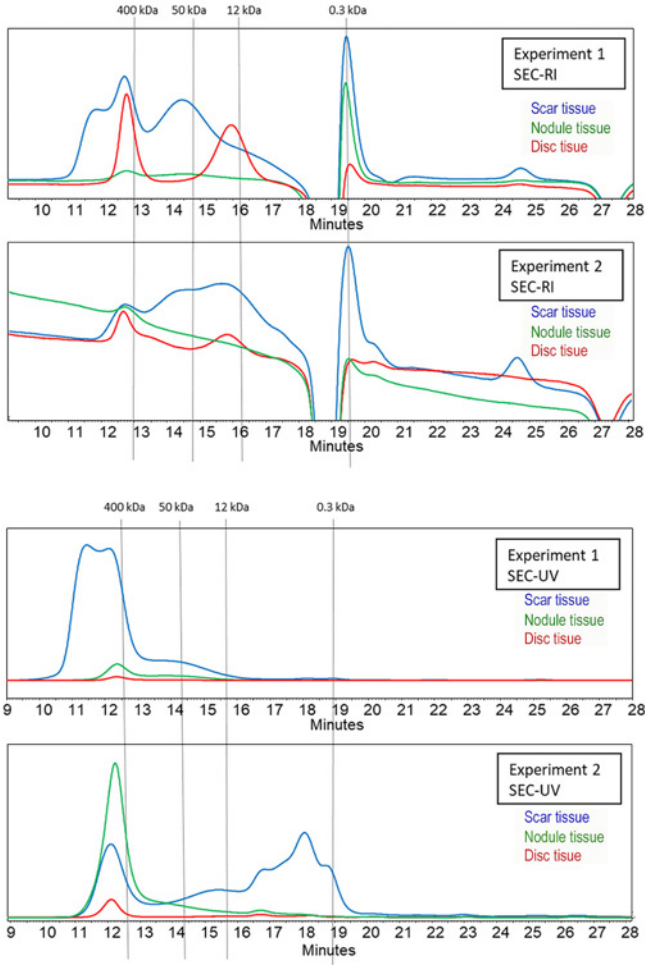

Figure 3. Size distribution of soluble macromolecules from scar, nodule, and disc tissues in two different experiments. The separation was followed by RI and UV-detection. In both experiments, the analyses of extracts of the scar tissue showed components in the molecular weight range 10-50 kDa by RI detection but not by UV. The presence of short-chain polysaccharides of hyaluronic acid can induce an inflammatory reaction.

Discussion

The present study demonstrated that there is a stronger resemblance between an experimentally induced disc herniation and scar tissue than between the induced disc herniation and nucleus pulposus tissue.

Ever since disc herniation was established as a clinical condition, it has been assumed that it is a result of hard disc tissue penetrating through the annulus fibrosus and immediately ready to mechanically deform an adjacent nerve root. However, this assumption was recently questioned[4]. Instead, it was demonstrated that after puncturing a lumbar disc in the rat, there was a leakage of nucleus pulposus. However, within the first minute after the puncture, the nucleus pulposus had been liquefied, and some weeks after the puncture, there was a small nodule formed over the puncture site that resembled a disc herniation. It was assumed that the formed nodule was the effect of intradiscal bioactive substances that had reached the epidural space contained in the leaking nucleus pulposus. This was later corroborated in a study showing that disc incision with nucleus pulposus or the application of nucleus pulposus onto the non-injured annulus fibrosus induced such nodule formation, whereas superficial annular incision without allowing nucleus pulposus leakage or application of autologous fat tissue did not[5]. It was then assumed that the formed nodule was more likely to be scar tissue than herniated nucleus pulposus. The present study was initiated to analyze the structural composition of this nodule and compare it to normal nucleus pulposus and scar tissue.

When performing the described procedure, there is always a disc herniation-like structure formed over the incision site. However, the size may vary from just a small bulge to a clear herniation-like structure. Most common (approximately 80%) is that there is a major herniation formed.

The proteomics assessment of nodule, scar, and disc tissues demonstrated that the nodule was more similar to scar

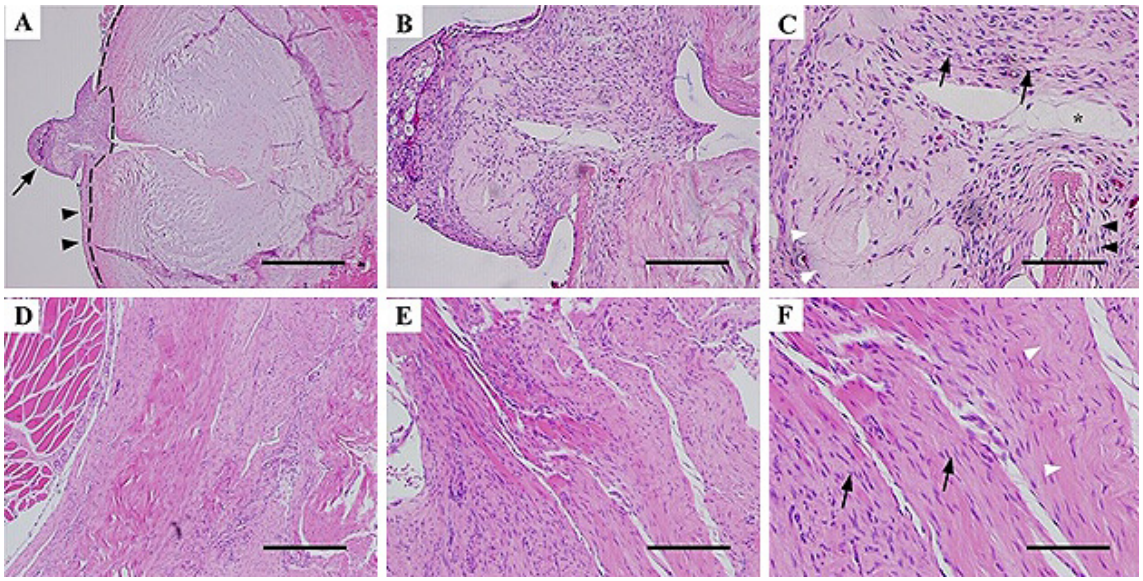

Figure 4. Hematoxylin and eosin stained sections of disc tissue and nodule (A-C) and scar tissue (D-F). Pictures are illustrated with 5x (A, D), 10x (B, E), and 20x (C, F) magnification. The arrow in A indicates the nodule and the arrow heads the superficial aspect of the annulus fibrosus. The dotted line indicates the border between the nodule (left) and the disc tissue (right) with nucleus pulposus in the center. The black arrow heads in C indicate the probable source of the nodule. The arrows in F indicate cells with fibroblast morphology, and the white arrow heads indicate ECM-like structures. Scale bars in A and D=25 μm; B and E=50 μm; C and F=100 μm.

tissue than to nucleus pulposus. Gene expression analysis showed that there was no resemblance between any tissues when looking at inflammatory genes but that, there was a clear resemblance between the nodule and scar tissue when analyzing ECM-related genes. Analysis of the GAG and polysaccharide size distribution revealed that all tissues contained polysaccharides, but only the nodule and scar tissues contained the shorter version, which could be short-chain hyaluronic acid that is known to induce inflammatory responses[7,8]. Finally, hematoxylin and eosin stained sections of the nodule, disc tissue, and scar tissue indicated that the morphology of the nodule and scar tissues is very similar with a majority of fibroblast-like cells and areas of what is probably ECM.

In summary, the newly formed nodule was found to be more similar to scar tissue than the herniated nucleus pulposus. However, it should be mentioned that these young, experimentally induced disc herniation-like nodules are not necessarily comparable to disc herniations found in adult humans. Such herniation tissue must also be assessed by the same technologies to verify any resemblance to these experimentally induced nodules. Of course, it might still be likely that many disc herniations, in fact, are herniated disc material when it comes to the clinical situation. We just feel intrigued that there may be other mechanisms for disc herniation formation.

It may seem only of academic interest to analyze the composition of these experimentally induced nodules. However, it is known that clinically established disc herniations may undergo spontaneous regression to a certain extent[9-12]. With this knowledge and the results from the present paper, one might think that it would be possible by pharmacological means to facilitate or monitor such regression. In fact, preliminary experimental observations indicate that this might be possible.

Conflicts of Interest: Kjell Olmarker is founder and part owner of Stayble Therapeutics AB, Mölndal, Sweden. No other benefits in any form have been or will be received from a commercial party related directly or indirectly to the subject of this manuscript.

Funding and Acknowledgement: The institution of the corresponding author (KO) has received funding from AFA Insurance, Stockholm, Sweden.

Author Contributions: All authors were involved in all 4 criteria for authorship as indicated by ICMJE.

References

1. Mixter WJ, Barr JS. Rupture of the intervertebral disc with involvement of the spinal canal. N Engl J Med. 1934;211:210-5.
2. Olmarker K, Rydevik B, Nordborg C. Autologous nucleus pulposus induces neurophysiologic and histologic changes in porcine cauda equina nerve roots. Spine. 1993;18(11):1425-32.
3. Olmarker K. Puncture of a lumbar intervertebral disc induces changes in spontaneous pain behavior: an experimental study in rats. Spine. 2008;33(8):850-5.
4. Olmarker K. Inflammatory mechanisms in disc related pain. ed. Helsinki: ORTON; 2007. LBP, controversies in clinical practice and research; p. 81-7.
5. Olmarker K. Puncture of a disc and application of nucleus pulposus induces disc herniation-like changes and osteophytes. An ex-

perimental study in rats. Open Orthop J. 2011;5:154-9.
6. Olmarker K, Myers RR. Pathogenesis of sciatic pain: role of herniated nucleus pulposus and deformation of spinal nerve root and dorsal root ganglion. Pain. 1998;78(2):99-105.
7. Lyle DB, Breger JC, Baeva LF, et al. Low molecular weight hyaluronic acid effects on murine macrophage nitric oxide production. J Biomed Mater Res A. 2010;94(3):893-904.
8. Litwiniuk M, Krejner A, Speyrer MS, et al. Hyaluronic acid in inflammation and tissue regeneration. Wounds. 2016;28(3):78-88.
9. Teplick JG, Haskin ME. Spontaneous regression of herniated nucleus pulposus. AJR Am J Roentgenol. 1985;145(2):371-5.
10. Lutman M, Girelli G. [Spontaneous regression of lumbar disk hernia]. Radiol Med. 1991;81(3):225-7.
11. Birbilis TA, Matis GK, Theodoropoulou EN. Spontaneous regression of a lumbar disc herniation: case report. Med Sci Monit. 2007;13(10):CS121-3.
12. Yang X, Zhang Q, Hao X, et al. Spontaneous regression of herniated lumbar discs: Report of one illustrative case and review of the literature. Clin Neurol Neurosurg. 2016;143:86-9.